

01 Nov 2009

## Characterisation and Mechanical Testing of Hydrothermally Treated HA/ZrO<sub>2</sub> Composites

D. J. Curran


T. J. Fleming

G. Kawachi

C. Ohtsuki

*et. al.* For a complete list of authors, see [https://scholarsmine.mst.edu/che\\_bioeng\\_facwork/1187](https://scholarsmine.mst.edu/che_bioeng_facwork/1187)

Follow this and additional works at: [https://scholarsmine.mst.edu/che\\_bioeng\\_facwork](https://scholarsmine.mst.edu/che_bioeng_facwork)

 Part of the [Biochemical and Biomolecular Engineering Commons](#), and the [Biomedical Devices and Instrumentation Commons](#)

### Recommended Citation

D. J. Curran et al., "Characterisation and Mechanical Testing of Hydrothermally Treated HA/ZrO<sub>2</sub> Composites," *Journal of Materials Science: Materials in Medicine*, vol. 20, no. 11, pp. 2235 - 2241, Springer, Nov 2009.

The definitive version is available at <https://doi.org/10.1007/s10856-009-3801-6>



This work is licensed under a [Creative Commons Attribution 4.0 License](#).

This Article - Journal is brought to you for free and open access by Scholars' Mine. It has been accepted for inclusion in Chemical and Biochemical Engineering Faculty Research & Creative Works by an authorized administrator of Scholars' Mine. This work is protected by U. S. Copyright Law. Unauthorized use including reproduction for redistribution requires the permission of the copyright holder. For more information, please contact [scholarsmine@mst.edu](mailto:scholarsmine@mst.edu).

# Characterisation and mechanical testing of hydrothermally treated HA/ZrO<sub>2</sub> composites

D. J. Curran · T. J. Fleming · G. Kawachi ·  
C. Ohtsuki · M. R. Towler

Received: 8 April 2009 / Accepted: 5 June 2009 / Published online: 13 June 2009  
© Springer Science+Business Media, LLC 2009

**Abstract** Hydrothermal treatment is traditionally employed to improve the sinterability of powder compacts by reducing porosity and increasing apparent density. The effect of hydrothermal treatment on green powder compacts has been assessed in order to better understand how treatment may affect the sinterability of the bodies. Laboratory synthesised nano sized hydroxyapatite (HA) and a commercial zirconia (ZrO<sub>2</sub>) powder have been ball milled together to create composite mixtures containing 0–5 wt% ZrO<sub>2</sub> loadings. Disc shaped bodies have been formed using uniaxial and subsequent isostatic pressure. The resultant coherent samples were subjected to hydrothermal treatment at either 120 or 250°C for 10 h in order to assess the effect of this processing technique on the physical, mechanical and microstructural properties of the green composites. ZrO<sub>2</sub> loadings up to 3 wt% increased apparent density from 90 to 92%, whereas increased loading to 5 wt% increased flexural strength, from 6 to 9 MPa. Increasing the hydrothermal treatment temperature increased open porosity, from ~44 to ~48% and reduced biaxial flexural strengths of the treated bodies compared to those of their room temperature isostatically pressed counterparts (~10 to ~6 MPa).

## 1 Introduction

The literature shows that dense ceramic bodies can be produced by a range of thermal treatments such as conventional [1, 2], microwave [3, 4] and spark plasma sintering [5, 6] but the application of high temperatures during processing may cause decomposition of the principal components. This is true for ceramic composites based on a hydroxyapatite (HA) matrix; a biomaterial employed in the repair of skeletal defects. Attempts have been made to improve the strength of HA by the incorporation of a second ceramic phase, such as ZrO<sub>2</sub> (e.g. yttria-doped tetragonal ZrO<sub>2</sub> polycrystals, Y-TZP), but this can have inherent disadvantages.

Sintering HA {Ca<sub>10</sub>(PO<sub>4</sub>)<sub>6</sub>(OH)<sub>2</sub>} at high temperatures can result in the formation of decomposition products such as tri-calcium phosphate, TCP {Ca<sub>3</sub>(PO<sub>4</sub>)<sub>2</sub>} and tetracalcium phosphate, TeCP {Ca<sub>4</sub>(P<sub>2</sub>O<sub>9</sub>)}. TeCP can decompose further to TCP and calcium oxide [CaO] at higher temperatures. These secondary phases have, in certain instances, been reported to adversely affect the biological response [7, 8].

When ZrO<sub>2</sub> is added to HA, high temperatures of 1200–1400°C are commonly required to sinter these composites to high density, but HA has been reported to be thermally unstable above 1300°C [5, 6]. It has commonly been observed that phase transformations/decompositions occur extensively during sintering of these composites at temperatures even below 1200°C. For example, at 1150°C, HA will react with the ZrO<sub>2</sub> phase, with the formation of cubic calcia-stabilised ZrO<sub>2</sub>, and subsequently calcium zirconate (CaZrO<sub>3</sub>) [9]. Increasing the sintering temperature further increases the amounts of β-TCP and CaZrO<sub>3</sub>. At a sintering temperature of 1400°C, virtually no HA remains and some α-TCP forms from β-TCP. This phase

---

D. J. Curran · T. J. Fleming · M. R. Towler (✉)  
Clinical Materials Unit, Materials and Surface Science Institute,  
University of Limerick, National Technological Park,  
Limerick, Ireland  
e-mail: Mark.Towler@ul.ie

G. Kawachi · C. Ohtsuki · M. R. Towler  
Department of Crystalline Materials Science, Graduate School  
of Engineering, Nagoya University, Nagoya, Japan

decomposition means that the theorised improvements in physical and mechanical properties associated with combining a high-strength, bioinert ceramic (Y-TZP) with the low-strength bioactive ceramic (HA) is lost. The problem of HA decomposition reactions in the presence of  $ZrO_2$  during sintering has limited the applications of these composites, as the mechanical and biological properties are compromised by the formation of these secondary phases.

The authors have previously shown that incorporating small quantities (up to 5 wt%) of  $ZrO_2$  in an HA matrix [10], and using nano-sized particles of the two phases [11], can retard reactions during synthesis, thereby minimising decomposition. However, there is still a desire for a novel technique to produce dense bodies that use lower temperatures in order to facilitate consolidation but eradicate any phase decomposition. Hydrothermal treatment [12, 13] may be one of these techniques which can form adhesions amongst solid phase powder compacts utilising a relatively low process temperature of around  $200^\circ\text{C}$ . The hydrothermal processing technique involves exposing samples to water vapour in an autoclave which is heated to the process temperature. Under hydrothermal conditions, the humidity level in the autoclave is 100%. This environment creates an equilibrium state between the liquid and vapour phase of the added water. Liquid water condenses on the exposed surfaces of the samples. It is expected that hydrothermal treatment of HA/ $ZrO_2$  composite powder compacts prior to sintering will produce unique porous microstructures.

With this in mind, research was conducted into the effect of hydrothermal processing on HA/ $ZrO_2$  composite green bodies [12, 13]. Hydrothermal techniques generally have less complicated reaction process compared to other consolidation techniques which should minimise potential decomposition of the HA matrix.

In order for a reaction to occur, HA must dissolve into the liquid water during the course of hydrothermal treatment. This continual solution/precipitation allows recrystallisation of HA to occur. However, HA possesses the lowest aqueous solubility of any of the calcium phosphates, which reduces further with increasing temperature. For this reason, other studies have not used HA as the starting material for this type of process but instead have used hydrothermal treatment to convert other CaP materials to HA.

In this procedure, cold isostatically pressed (CIP'd) bodies of HA and  $ZrO_2$  particles were produced to determine if the low temperatures employed during the novel hydrothermal process caused densification of the bodies to occur and increase the mechanical properties without subsequent decomposition of the pure HA phase.

## 2 Methods

### 2.1 Nano-sized HA and $ZrO_2$ powders

Samples of pure HA were produced at a synthesis temperature of  $25^\circ\text{C}$  by a simple precipitation method [14]. A dilute solution containing 78.72 g Analar grade di-ammonium hydrogen orthophosphate (Fisher Scientific, Ireland), made basic by the addition of 10 ml of Analar grade ammonium hydroxide (Fisher Scientific, Ireland), was added to a dilute solution containing 26.41 g Analar grade calcium nitrate (BDH supplies, Leicestershire, UK), also made basic by the addition of 25 ml of Analar grade ammonium. Addition was by a dropping funnel, taking one hour for completion, and the sample was then left to stand (24 h;  $25^\circ\text{C}$ ). After standing, the suspension had separated, and the clear aqueous layer was decanted, then the remaining slurry was washed with distilled water, re-stirred and left to stand again. This procedure was undertaken three times, to remove any unwanted residue from the sample. The suspension was then filtered and the filter-cake was washed and filtered again until most of the water had been removed and then placed into a beaker and dried in an oven ( $85^\circ\text{C}$ , 20 h). The resulting dried powder was ground (pestle and mortar) and passed through a  $90\ \mu\text{m}$  sieve to remove agglomerates.

#### 2.1.1 Particle size analysis

A Malvern Mastersizer 2000 (Malvern Instruments Ltd., Malvern, UK) was employed to measure the particle size of the HA. Approximately 25 ml of the HA suspension was added drop wise to the sample tank, which was filled with distilled water, resulting in a measured obscuration of approximately 9%. The solution was subject to ultrasonic and mechanical agitation for the duration of the measurement cycles in order to eliminate any agglomerates and to ensure even dispersion throughout the sample tank. Ten individual measurements were made for each sample. The particle size distribution (median particle size,  $D_{50}$ , along with the diameter of the particles at 10%,  $D_{10}$ , and 90%,  $D_{90}$ , of the cumulative frequency curve) were recorded.

#### 2.1.2 Surface area analysis

The surface area of the HA powder was evaluated using the BET method (Micrometrics ASAP 2010, USA) utilising nitrogen as the absorbate. The samples were de-gassed overnight at  $120^\circ\text{C}$  under vacuum.

### 2.1.3 Ca:P ratio

The calcium to phosphorus ratio and the trace element impurity content of the laboratory synthesised HA were determined by X-ray fluorescence (Ceram Research Ltd., Stoke on Trent, UK).

Following powder characterisation and the addition of  $ZrO_2$ , samples were pressed (Sect. 2.1.4) and hydrothermally treated (Sect. 2.1.5).

### 2.1.4 Production of green bodies

The HA was then ball milled (6 h) along with the appropriate amount of  $ZrO_2$  powder (99.9% purity, Tosoh Corporation, Japan), of known particle size and specific surface area, in order to produce homogeneous lots with 0, 1, 3 and 5 wt%  $ZrO_2$  loadings.

The composite powders were weighed out in 1 g batches and then subjected to uniaxial pressure of 150 MPa in a 20 mm  $\varnothing$  stainless steel die followed by cold isostatic pressing (CIP) at 200 MPa to eliminate internal density gradients. These bodies were then subjected to the hydrothermal treatment.

### 2.1.5 Hydrothermal treatment technique

Green bodies were placed in a 100 cm<sup>3</sup> autoclave with 20 cm<sup>3</sup> of distilled water. Samples were rested on a Teflon stage to separate them from the water (Fig. 1). Samples were treated hydrothermally at either 120 or 250°C for 10 h under saturated vapour pressure;  $n = 5$  for each temperature.

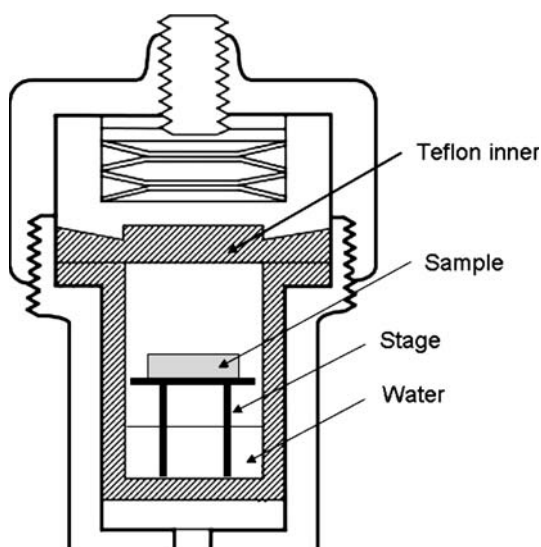


**Fig. 1** Schematic illustration of sample setting during hydrothermal treatment

After hydrothermal treatment, samples were washed and oven dried (100°C, 6 h, in air).

### 2.1.6 Consolidated body characterisation

The bodies were then characterised by powder X-ray diffraction (XRD; Rigaku, Rint2100, Japan) with graphite-monochromatised Cu K $\alpha$  radiation, operating at 40 kV and 20 mA, to identify phases present, and Scanning Electron Microscopy (JOEL, JSM-5600, Japan) at 15 kV on the surfaces of the samples to determine the presence of consolidation.

The density and porosity of the CIP'd bodies was measured using an Archimedes technique whereby the bodies were boiled in water. Post hydrothermal treatment the samples were left to dry for several days and again the density and open porosity was assessed using an Archimedes method in water under vacuum.

## 2.2 Mechanical testing

The CIP'd and hydrothermally treated bodies (both unfilled and  $ZrO_2$  loaded) were mechanically tested to determine biaxial flexural strength (BFS, Sect. 2.2.1). Microhardness (Sect. 2.2.2) was also evaluated and fracture surface morphologies were analysed by SEM (Sect. 2.2.3).



**Fig. 2** Assembled ASTM F 394 test jig, no specimen installed

### 2.2.1 Biaxial flexural strength

BFS was measured using a modification of ISO 6872/ASTM F394 employing a bi-axial flexural strength test jig, a 500 N load cell and a load frame (Lloyd Instruments Limited LR50 K) operating at a 1 mm/min crosshead speed. The jig consists of three 2 mm  $\varnothing$  ball bearings sitting 120° apart on the circumference of an 8 mm  $\varnothing$  support circle onto which the sample sits (Fig. 2). A load is applied perpendicular to the sample along the central axis of the support circle through a stainless steel ball bearing (2.1 mm  $\varnothing$ ). Five samples of each composition were tested. The load/displacement and load at fracture are recorded and used along with the Poisson's ratio of the material to calculate the BFS.

### 2.2.2 Fracture surface evaluation

SEM was performed on the fracture surfaces resulting from bi-axial flexural strength testing. Post fracture, the samples were mounted in retention clips to ensure that the fracture surface was perpendicular to the scanning beam. The fracture surfaces were then gold sputtered and imaged using a JOEL JSM 840 (JEOL, Japan) with an accelerating voltage of 20 kV.

## 3 Results

### 3.1 Laboratory synthesised HA

The laboratory synthesised HA had a mean particle size of 0.192  $\mu\text{m}$ , a specific surface area of  $151.4711 \pm 0.1587 \text{ m}^2/\text{g}$  and a Ca:P ratio of 1.66, close to that of stoichiometric HA (Ca:P, 1.67). The Tosoh sourced  $\text{ZrO}_2$  had a mean particle size of 0.166  $\mu\text{m}$ . Post ball milling a typical composite powder had a mean particle size of Q  $\mu\text{m}$  (Table 1).

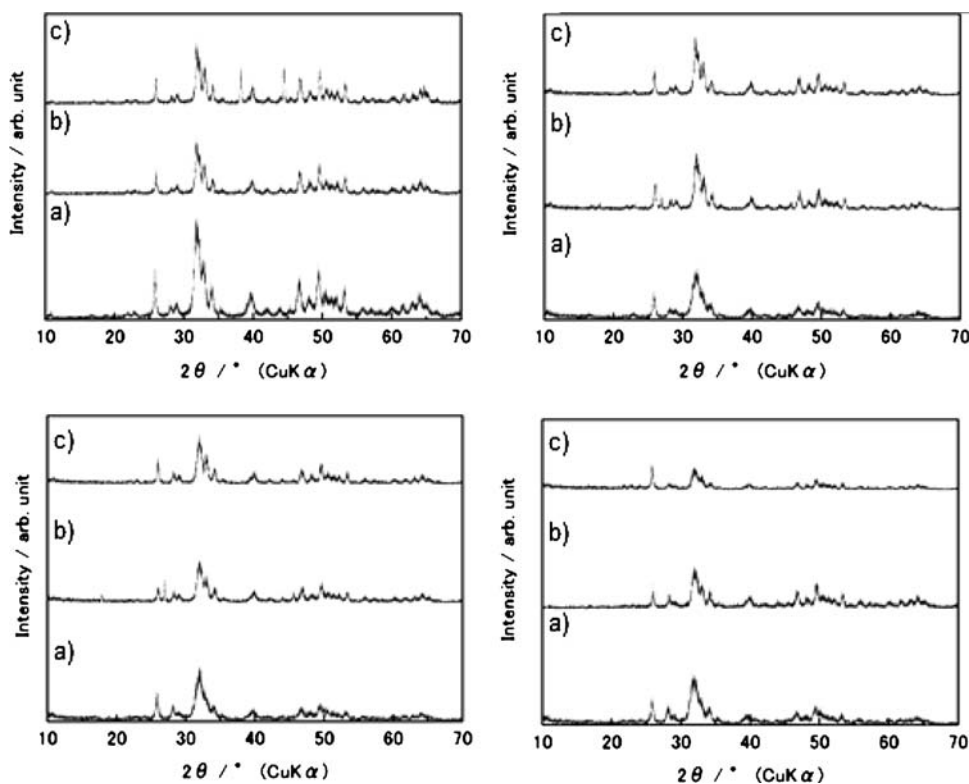
### 3.2 X-ray diffraction

The X-ray diffraction data of the hydrothermally treated samples consisting of laboratory HA and lab HA composites with 0, 1, 3 and 5 wt% are presented in Fig. 3. The

**Table 1** Physical properties of powder materials

	Ca/P ratio	Mean particle size ( $\mu\text{m}$ )
Synthesised HA	1.66	0.192
Tosoh $\text{ZrO}_2$	–	0.166
Typical composite	–	–

**Fig. 3** The X-ray diffraction patterns of hydrothermally treated laboratory synthesised hydroxyapatite (*top left*), with 1 wt%  $\text{ZrO}_2$  addition (*top right*), 3 wt%  $\text{ZrO}_2$  addition (*bottom left*) and 5 wt%  $\text{ZrO}_2$  addition (*bottom right*); **a** prior to hydrothermal treatment, **b** hydrothermally treated at 120°C for 10 h, **c** hydrothermally treated at 250°C for 10 h



diffractograms clearly indicate that hydrothermal treatment increases the relative intensity of the peaks. This indicates that the treatment increases the crystallinity of the CIPd bodies. This suggests that some form of recrystallisation has occurred despite the limited solubility of HA.

According to the X-ray diffraction data of both the treated and untreated HA, the only phase present is HA (09-0432), indicating that the phase of the material is unchanged by hydrothermal treatment. Ca-deficient HA ( $Ca/P < 1.67$ ) can decompose into stoichiometric HA ( $Ca/P = 1.67$ ) and  $\beta$ -Tricalcium phosphate ( $Ca/P = 1.50$ ). If  $PO_4$  deficient HA ( $Ca/P > 1.67$ ) e.g. HA containing carbonate ions, it decomposes into stoichiometric HA ( $Ca/P = 1.67$ ) and CaO. There is no indication of  $\beta$ -Tricalcium phosphate or CaO in any of the X-ray diffraction data which indicates that all tested samples were stoichiometric HA ( $Ca/P = 1.67$ ) [15].

### 3.3 Density and open porosity

From Fig. 4, the apparent density of the CIPd samples is 86–87% of the HA/ $ZrO_2$  composite theoretical density (TD) regardless of the amount of  $ZrO_2$  added. The hydrothermally treated materials follow a similar trend to their untreated counterparts but exhibit increased densities. The materials treated at 120°C possess 90–91% TD whereas the materials treated at 250°C experience an increase of ~1% with respect to those treated at 120°C, i.e. between 91 and 92% TD. The composites containing 3 wt%  $ZrO_2$  possess the highest densities and least variation regardless of processing temperature.

The open porosity values of the composite materials are presented in Fig. 5. The open porosity values of the CIPd materials decrease linearly, within standard deviations, with increasing  $ZrO_2$  content. The undoped material possesses ~44% open porosity which decreases to 42% with

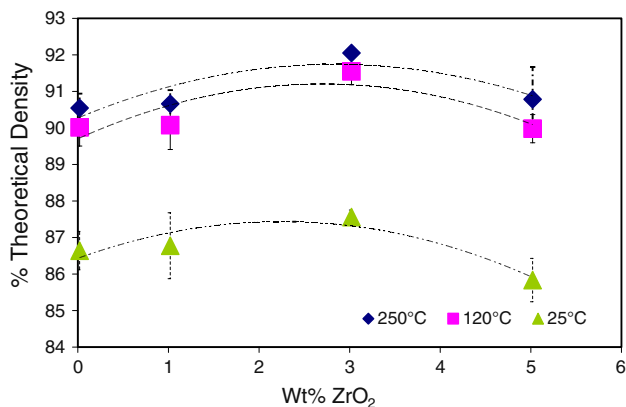


**Fig. 4** Theoretical densities of HA- $ZrO_2$  composites hydrothermally treated at three different temperatures

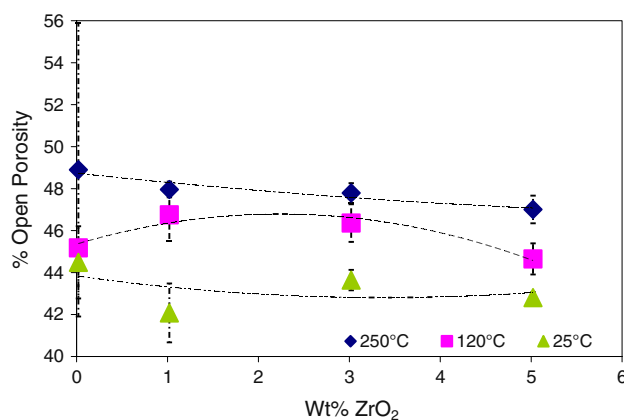


**Fig. 5** Open porosities of HA- $ZrO_2$  composites hydrothermally treated at three different temperatures

the addition of 5 wt%  $ZrO_2$ . The undoped HA treated at 120°C possesses an open porosity of 45%, which rises to 47% with the addition of 1 wt%  $ZrO_2$ . Increasing  $ZrO_2$  serves to reduce open porosity in a linear fashion, returning to 45% with 5 wt%  $ZrO_2$ . The open porosity of the materials treated at 250°C decrease linearly from 49 to 46% on going from 0 to 5 wt%  $ZrO_2$  content. There is a clear delineation in values with increased processing temperature resulting in increased open porosity values at every  $ZrO_2$  loading.

### 3.4 Biaxial flexural strength

BFS values of the composite bodies are presented in Fig. 6. Between 0 and 3 wt%  $ZrO_2$ , The BFS of the CIPd materials ranges from 11 to 13 MPa, whereas the strengths of the hydrothermally treated samples range from 5 to 7 MPa. All the composites containing 5 wt%  $ZrO_2$  possess BFS of ~9 MPa.

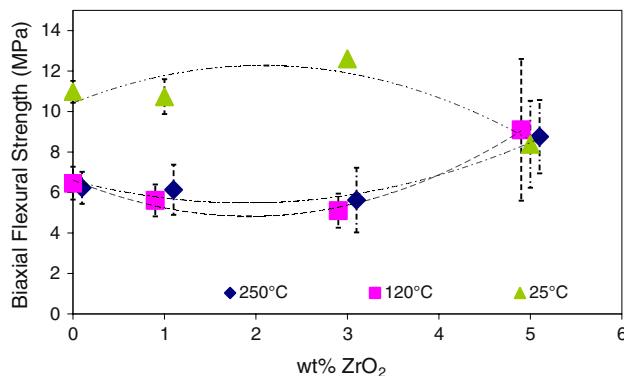


**Fig. 6** Biaxial flexural strength vs  $ZrO_2$  content for CIPd and hydrothermally treated samples

**Fig. 7** SEM micrographs (500 $\times$ ) of HA at room temperature (*top left*) and hydrothermally treated at 120°C (*top right*) and 250°C (*bottom centre*)

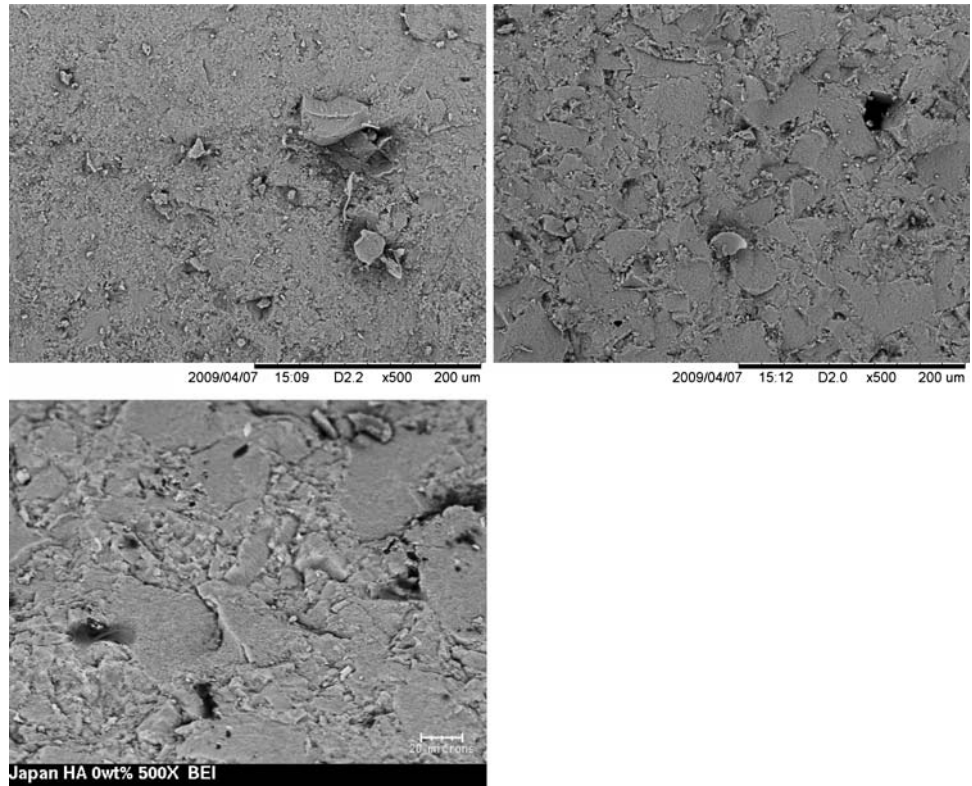
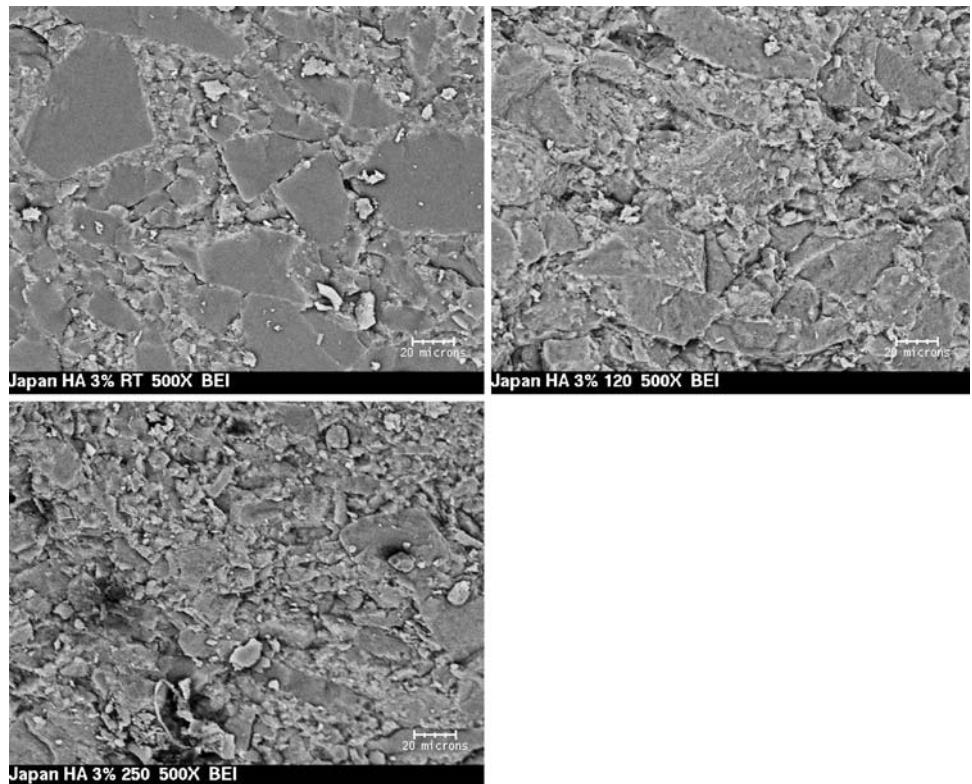


**Fig. 8** SEM micrographs (500 $\times$ ) of 3 wt% ZrO<sub>2</sub>/HA composites at room temperature (*top left*) and hydrothermally treated at 120°C (*top right*) and 250°C (*bottom*)



### 3.5 Scanning electron microscopy

Back scattered electron images of the fracture surfaces of the compositions which exhibit extremal values in bi-axial flexural strength values (0 and 3 wt% ZrO<sub>2</sub> loading) are presented in Figs. 7 and 8.

From Fig. 7 it is evident that the amount and size of trans-granular fracture surfaces increases with increased hydrothermal processing temperature. From Fig. 8 it can be seen that for composites containing 3 wt% ZrO<sub>2</sub> the amount of inter-granular fracture surfaces increases with increasing hydrothermal processing temperature. The difference in fracture mechanisms between Figs. 7 and 8 may be due to the interaction of ZrO<sub>2</sub> with the HA matrix.

## 4 Discussion

The effect of hydrothermal treatment on HA/ZrO<sub>2</sub> composite green bodies has been investigated. Preliminary results suggest that hydrothermal treatment does offer some consolidation to the ceramic bodies as demonstrated in Fig. 4 (as compared to the CIPd samples). This consolidation is a surface recrystallisation effect which in turn increases the size of the existing voids and pores. The increased defect size has the effect of reducing the treated green bodies' strengths.

It is not unreasonable to assume that the reduced open porosity and increased apparent density of the treated bodies results in the improved sinterability reported in the literature.

As there is no thermal gradient present within the autoclave, an equilibrium condition exists between the liquid and vapour phases of the added water, implying that the exposed surfaces of the bodies are in contact with liquid water during the course of hydrothermal treatment. It is expected that some of the HA particles used in this study, although possessing low solubility, dissolve and later precipitate. Due to the reprecipitation and recrystallisation of HA, only the accessible surfaces of sample e.g. the surfaces of the open porosity, were modified.

The re-precipitation of HA in the saturated water vapour environment of the autoclave leads to the conversion of non stoichiometric HA (as indicated by the Ca:P ratio of 1.66 of the precipitated powders) to stoichiometric HA as indicated by the absence of additional phases in the X-ray diffractographs of the hydrothermally treated bodies.

Increased ZrO<sub>2</sub> content, up to 3 wt%, increased apparent density and open porosity of the composites which, in turn, reduced BFS due to the increase in the number of critical flaws, though these samples exhibit increased reliability as indicated by the narrower range of standard deviations. This modification in microstructure with respect to the CIPd material is reflected in the SEM micrographs.

## References

- Bettinelli A, Guille J, et al. Densification of aluminas at 1400°C. *Ceram Intl.* 1998;14(1):31–4.
- Kingery WD, Bowen HK. *Introduction to ceramics*. New York: Wiley; 1976.
- Cheng JP, Agrawal D, et al. Microwave sintering of transparent alumina. *Mater Lett.* 2002;56(4):587–92.
- Upadhyaya DD, Ghosh A, et al. Microwave sintering of zirconia ceramics. *J Mater Sci.* 2001;36(19):4701–7.
- Kumar R, Prakash KH. Microstructure and mechanical properties of spark plasma sintering zirconia-hydroxyapatite nano-composite powders. *Acta Mater.* 2005;53(8):2327–35.
- Que W, Khor KA, et al. Hydroxyapatite/titania nanocomposites derived by combining high-energy ball milling with spark plasma sintering processes. *J Eur Ceram Soc.* 2005;28:3083–90.
- Nagarajan VS, Rao KJ. Structural, mechanical and biocompatibility studies of hydroxyapatite-derived composites toughened by zirconia addition. *J Mater Chem.* 1993;3:43–51.
- Hing KA, Gibson IR, Di-silvio L, Best SM, Bonfield W (1998) Effect of variation of Ca:P ratio on the cellular response of primary human osteoblast-like cells to hydroxyapatite based ceramics. In: LeGeros RZ, LeGeros, JP, editors. *Proceedings of the 11th international symposium on ceramics in medicine*. New York: World Scientific Publishing Co; 1998. pp. 293–296.
- Rao WR, Boehm RF. A study of sintered apatites. *J Dent Res.* 1974;53:1351–4.
- Towler MR. *Processing, characterisation and mechanical properties of hydroxyapatite-zirconia composites for skeletal implants*. London: University of London; 1997.
- Towler MR, Gibson IR, Best SM. Novel processing of hydroxyapatite-zirconia composites using nano-sized particles. *J Mater Sci Lett.* 2000;19(24):2209–11.
- Xin-bo X, Xie-rong Z, Chun-li Z. Preparation of enhanced HA coating on H<sub>2</sub>O<sub>2</sub>-treated carbon/carbon composite by induction heating and hydrothermal treatment methods. *Mater Chem Phys.* 2009;114(1):434–8.
- Ji S, Murakami S, Kamitakahara M, Ioku K. Fabrication of titania/hydroxyapatite composite granules for photo-catalyst. *Mater Res Bull.* 2009;44(4):768–74.
- Jarcho M, Bolen CH, Thomas MB, Bobick J, Kay JF, Doremus RH. Hydroxylapatite synthesis and characterisation in dense polycrystalline form. *J Mater Sci.* 1976;11:2027–35.
- Kunio Ishikawa PD, Shulamic R. Determination of the Ca/P ratio in calcium-deficient hydroxyapatite using X-ray diffraction analysis. *J Mater Sci: Mater Med.* 1993;4(2):165–8.